



## SPATIO-TEMPORAL MAPPING OF SOLAR ENERGY POTENTIAL OF DUTSE, JIGAWA STATE NIGERIA USING ARCGIS SOLAR RADIATION SPATIAL ANALYST TOOL

Idi, B. Y.

Department of Physics, Federal University Dutse, Jigawa State, Nigeria  
belyus2000@gmail.com

### ABSTRACT

*Efficient solar energy harnessing technology is required for sustainability and effective utilization of the resource. In this work, a survey of solar energy potential of Dutse, Jigawa state Nigeria was carried out with the aim of identifying the best location for optimal performance of solar energy power plant. Elevation information of the study area was obtained from Google Earth's Digital Elevation Model (DEM) data collected by NASA's Shuttle Radar Topography Mission (SRTM). With the DEM and the solar constant as inputs, ArcGIS's solar radiation analyst tool was used to estimate the effect of topography and its related parameters (slope, aspect, hillshed, viewshed) on both direct and diffuse solar radiation leading to an area solar insolation map for both the direct and diffuse components. Total insolation map was computed for the 12 months of the year 2017. The insolation map for the whole year varies significantly from 0.080 kWhm<sup>-2</sup> to about 2,684.358 kWhm<sup>-2</sup>. Two regions receiving maximum insolation were identified: mountainous region 1 km east of Mopol Barrack and the western end of the town, about 7.5 km east of Jidawa Lake. The temporal analysis of the monthly insolation showed that peak value was recorded in the month of April while minimum values were recorded in the months of December and January. The two regions are therefore recommended as the best location for optimal performance of solar power generating plant.*

**Keywords:** Solar Energy; Solar Insolation; Solar Radiation; Spatial Analyst; Dutse.

### INTRODUCTION

Solar is a non-dispatchable, highly variable but fairly predictable energy source that depends on many complex spatial and temporal variables. This is owing to the variation of the intensity of solar insolation incident on the earth surface with location (latitude), season, day of the month, time of the day, cloud cover and other climatic and environmental factors. The incident solar radiation (insolation) is the fundamental source of energy to the earth and therefore the driving force for the earth's physical, chemical and biological activities. The mean annual radiation intensity incident on a spherical earth model perpendicular to the sun's rays at the edge of the earth surface, the solar constant is about 1370W/m<sup>2</sup> and varies greatly by about ±25%. (Li *et al.*, 2011) due to the spatial and temporal variation in the distribution of insolation. Temporal variation occurs with latitude, times of the day, variation in earth-sun distance with times of the year and cloud cover.

The spatial variation occurs due to the spatial variation in topography and landscape of the earth surface. On a spatial scale, topography is a major factor that determines

the spatial variability of the solar insolation. While elevation of a point on the earth surface determines the mean earth-sun distance of the point, the orientation of the surface (slope, aspect) regulate the shadows cast by the topographic features on the point thereby modifying the total insolation at the point (Kumar, *et al.*, 1997). The atmospherically modified incoming solar radiation incident on the earth surface is made up of three components (Hetrick, *et al.*, 1993), direct, diffuse and reflected components. The sum of these three, referred to as global solar insolation, is the total radiation received at a point. The spatio-temporal variability of this quantity leads to high spatial and temporal heterogeneity in the availability of solar energy. Solar insolation of a given area is a relevant parameter being a measure of the solar energy potential of the area. For optimal performance, solar energy, devices should be sited in an area of high insolation. Studying and mapping the spatial variability of solar insolation of a given area will therefore be used to identify the most suitable location for solar power plant.

In this work, solar radiation analyst tools of the ArcGIS Spatial Analyst extension was used to analyze the effect of topography and its related parameters, notably slope, aspect and hillshade on solar insolation of an area characterized by gently undulating landform. The main objective of the work is to produce insolation map of the area and identify the most suitable location for siting solar power plant. The work intends to complement the Nigerian government's effort toward optimal harnessing of solar power as environmentally friendly alternative energy resource.

**MATERIALS AND METHODS**

**Theoretical framework**

Analyst extension tool is a Geographic Information System (GIS) based solar radiation modeling extension of ESRI ArcGIS developed based on Fu and Rich (1999) solar radiation modeling algorithm on ArcView platform. The tool computes insolation map using Digital Elevation Model (DEM) as input by taking into account the influence of latitude, elevation, steepness (slope), surface orientation (aspect), shadow cast by surrounding topography (viewsheds), sunshine hours, the sun angle (zenith) and the atmospheric effect (Effat, 2016). Solar radiation computation begins with a solar constant and then account for the atmospheric effects based on transmittivity, air mass depth, sunshine hours and elevation.

Solar insulations at a point is the intercepted radiation received at the point due to direct, diffuse and reflected components of radiation and is therefore the sum of these three components. The reflected component is however considered negligible for many purposes (Rich, 1990). Direct radiation is a function of solar angle, and the topographic viewshed. Direct solar radiation intensity  $I_{dir}$  is given in term of solar constant  $S_0$  by Gates (1980) as

$$I_{dir} = S_0 \tau^m \cos i \tag{1}$$

Where  $\tau$  is the atmospheric transmittance for the shortest path in the direction of the zenith,  $m$  is the air mass ratio, the ratio of the path length in the direction of the sun and  $i$  is the solar ray incident angle with respect to the

plane of interception. The atmospheric transmittance varies with wavelength of the radiation. A value of 0.6 averaged over all wavelengths recommended by Gates (1980) was used in ArcGIS Solar Analyst tool. The air mass ratio is a measure of the direct optical path length through the atmosphere relative to the vertically upward path length. Thus it is geometrically related to the zenith angle  $z$  as (Wüffel, 2005).

$$m = \frac{1}{\cos z} \tag{2}$$

The solar incident angle  $i$  is the angle of incidence between the solar rays and normal to the plane of interception and is given by Gates (1980) as

$$\cos i = \sin \theta \cos \alpha \cos(\alpha - \alpha_s) + \cos \theta \sin \alpha \tag{3}$$

where  $\theta$  is the surface slope,  $\alpha$  is the elevation angle of the sun,  $\alpha_s$  is the solar azimuth angle and  $\alpha_s$  is the aspect of the surface.

The diffuse insolation  $I_{dif}$  is also computed based on the solar constant, taking into consideration the diffusion coefficient  $\tau_d$  as given by Gates (1980) as

$$I_{dif} = S_0 \tau_d \cos^2 \left( \frac{\theta}{2} \right) \sin \alpha \tag{4}$$

Diffusion coefficient increases with decrease in the scattering coefficient  $\tau$  and the two are related by the equation (Kumar et al., 1997)

$$\tau_d = 0.271 - 0.29 \tau^m \tag{5}$$

The global insolation is the sum of the direct and diffuse insulations.

**Study area**

The study covered a 360 km<sup>2</sup> enclosing Dutse, Jigawa state and its surroundings (Fig. 1) geographically bound by lower left coordinate 9.255669°E, 11.617295°N and upper right coordinate 9.421609°E, 11.804351°N at an average elevation of about 434 m above mean sea level. The area is geologically within the Precambrian basement complex of north central Nigeria (Obaje, 2009) and is therefore characterized by diverse landforms with few elevated landscape features of igneous rocks surrounded by relatively flat landscape.

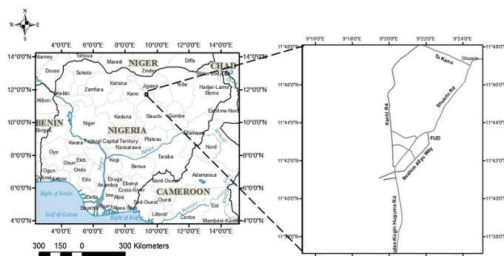


Fig. 1. Map of Nigeria showing the study area

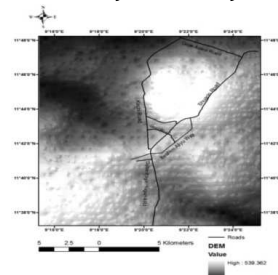


Fig.2. Digital Elevation Model (DEM) of the study area based on Google earth's elevation data

The input data for this work is the DEM raster image of the study area. Elevation data was obtained from Google earth software. Digitizing Google Earth image of a specific area with a point feature gives 3-D coordinates of the points (longitude, latitude and elevation). Comparison of Google Earth and GPS elevation data by Mohammed, et. al (2013) gives an RMS value of 1.73m. DEM raster of the area was plotted using the acquired elevation data. Fig. 2 gives the DEM produced with the Google earth acquired elevation data.

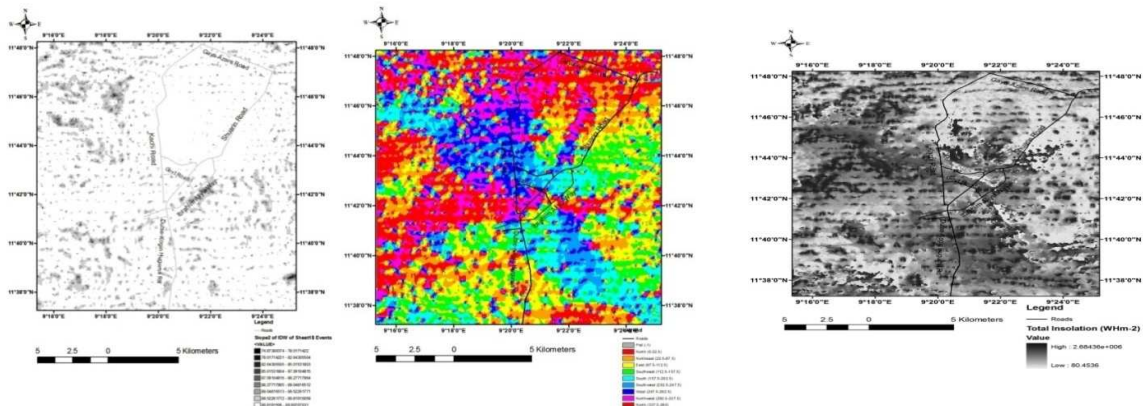
The DEM map was used to compute the viewshed map, which is a map depicting a view of the visible sky and its direction obstructed by the surrounding topography and surface features. The viewshed computation involves computation of solar horizontal angles for certain number of directions which are plotted as a hemispherical representation of the sky. The viewshed map is then overlaid separately on direct sunmap and a diffused sky map. The sunmap is a raster image representing the position of the sun at different hours of the day through the days of the year in a hemispherical projection. It is made up of discrete sectors defined by the position of the sun at different times of the day throughout the year determined by the coordinates of the location. The position of each sector in the map is determined by the zenith and azimuth of its centre. Solar radiation originating from each sector, as affected by the zenith and azimuth, is computed and displayed accordingly. Skymap is also constructed by dividing the sky into series of sectors of different zenith and azimuth angles. Diffuse radiation can be computed with either uniform model in which incoming diffuse radiation is considered uniform or standard overcast model in which diffuse radiation flux varies with zenith angle (Percy, 1989). In this work, standard overcast model was implemented.

In this work, area solar radiation method was used to compute the global insolation map of the area at 9.269463°N for the year 2017 starting from the 1<sup>st</sup> to 365<sup>th</sup> day of the year at a daily interval of 14 days and 30 min (0.5 hour ) hourly interval. Thus based on the input data, the Area Solar radiation tool computes the biweekly solar insolation for every location of the area from the 1<sup>st</sup> to the last day of the year 2017. Temporal variation of the global insolation was studied by computing the monthly global solar area insolation for each month of the year 2017. The computation was based on the number of days of the month at an interval of 0.5 day. Using the latitude information, the tool computes the global insolation for the months taking into consideration the zenith, azimuth and slope information.

**RESULTS**

In line with physical observation, the raster images of topographic parameters obtained from this work have shown that the area is generally made up of gentle slopes in various directions. Fig 3(a and b) are the plots of the slope and aspect of the area. While slope defines the landscape of the area, aspect describes the orientation of the landform. It is evidently clear from the maps that the visibility is determined by the slope, but slope orientation is a significant factor. The global insolation is obtained as the raster sum of the direct and diffuse radiation. Fig.3(c) is the raster plot of the global insolation obtained for the sampled period.

Significant variability in the spatial distribution of the global insolation is evidently observable from the map. Table 1 gives the statistical analysis of the computed global insolation within the study area. Fig.4 is the histogram plot of the monthly global insolation for the area.



(a) Slope (b) Aspect (c) Global  
 (b) Fig. 3: (a) Slope, (b) Aspect and (c) Global Insolation map.

Table 1. Global insolation distribution statistics

Minimum	0.080 kWhm <sup>-2</sup>
Maximum	2,684.358 kWhm <sup>-2</sup>
Mean	1108.065 kWhm <sup>-2</sup>
Standard Deviation	692.119 kWhm <sup>-2</sup>

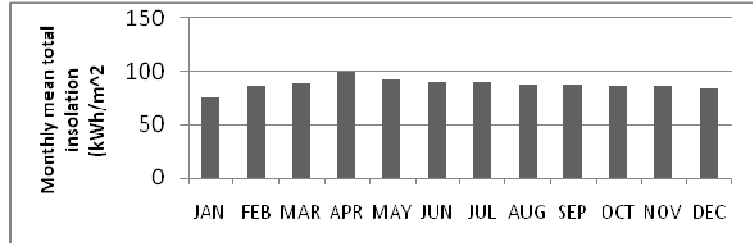


Fig. 4 Monthly distribution of global insolation for the year 2017

The results show that a maximum value of 99.872 kWhm<sup>-2</sup> was obtained in the month of April while a minimum of 75.170 kWhm<sup>-2</sup> was recorded for the month of January within the sampled period. The plot shows that monthly variation in the distribution of global insolation for the area is not very significant.

**DISCUSSION**

The results of this study showed significant variability in the spatial distribution of insolation. Close observation of raster images indicate a relationship between the spatial distributions of insolation with slope orientation. Comparison of Fig. 3(b) with Fig. 3(c) showed that south and southeast - facing slopes received the highest global insulations while minimal insolation is received by the north and northwest-facing slopes. Southeast facing slopes have corresponding azimuth angles within a range of 90° - 180° while northwest - facing slopes have higher azimuthal angles (270°-360°). This therefore indicates that slope orientation is an important factor in spatial distribution of solar radiation energies.

The results of the monthly temporal distribution of the global insolation showed that peak is recorded in the month of April while minimum is recorded in the month of January. (Fig.4). This can be explained based on the relationship between the sun path, defined by the time- varying solar elevation and the solar azimuth angle. Analysis of the solar chart of the study area obtained from University of Oregon Solar Radiation Monitoring Laboratory database (OU, 2007) showed that the curve representing the month of April has the highest solar elevation and stays at a minimum elevation of 75° from 11.00 a m to 1.00 p m each day, with a peak of 90° at noon. The curves representing the months of January and December on the

other hand have the lowest solar elevation for all times of the days.

Spatial analysis of Fig. 3(c) in comparison with the geographic map of the study area showed that maximum global solar insolation of about 2,684.358 kWhm<sup>-2</sup> is received at two different locations within the area. They are identified as hilly igneous rock outcrop region 1 km east of Mopol Barrack with centre coordinates 9.341869°E, 11.734908°N and the western end of the town, about 7.5 km east of Jidawa Lake with centre coordinates 9.291045°E, 11.741342°N . The two regions are therefore recommended as the best location for optimal performance of solar power generating plant.

**CONCLUSION**

The performance of solar energy devices is obviously dependent on the amount of solar insolation received and therefore varies with geographic location. Large scale high resolution solar insolation measurement provides an important data for application in the fields of renewable energy, agriculture, forestry etc. Direct field measurement could not provide the needed resolution on a landscape scale. In this work, an effective tool for a large spatial scale assessment of solar insolation of an area is demonstrated. ArcGIS Solar Analyst tool has the capability of estimating the insolation of area at the spatial resolution of a satellite image. From the foregoing, spatial distribution of direct, diffuse and global insolation of Dutse, Jigawa state Nigeria and its surroundings were mapped leading to the identification of the most suitable location for optimal performance of solar power devices. The tool therefore has wide range of application in renewable energy generation, precision agricultural activities, conservation and ecological studies.

**REFERENCES**

Effat, H. A. (2016). Mapping Solar Energy Potential Zones, using SRTM and Spatial Analysis, Application in Lake Nasser Region, Egypt. *International Journal of Sustainable Land Use and Urban Planning*, 3(1): 1-14.

Fu, P. and Rich, P.M. (1999). Design and implementation of the Solar Analyst: an ArcView extension for modeling solar radiation at landscape scales. *Proceedings of the Nineteenth Annual ESRI User Conference*.

**Special Conference Edition November, 2017**

- Gates, D.M. 1980. *Biophysical Ecology*. Springer-Verlag. New York
- Hetrick, W.A., Rich, P.M., Barnes, F.J., and Weiss, S. B. (1993). GIS-based solar radiation flux models. *American Society for Photogrammetry and Remote Sensing Technical Papers*, 3:132-143.
- Kumar, L., Skidmore, A. K. and Knowles, E. (1997). Modelling topographic variation in solar radiation in a GIS environment. *International Journal of Geographical Information Science*. 11(5): 475-497.
- Li, H., Lian, Y., Wang, X., Ma, W., Zbao, L. (2011). Solar constant values for estimating solar radiation. *Energy*, 36(3):1785-1789.
- Mohammed, N. Z., Ghazi, A. and Mustafa, H. E. (2013). Positional Accuracy Testing of Google Earth. *International Journal of Multidisciplinary Sciences and Engineering*, 4(6): 6-9.
- Obaje, N. G. (2009). *Geology and Mineral Resources of Nigeria Lecture Notes in Earth Sciences*. Springer, Springer-Verlag Berlin Heidelberg.
- Pearcy, R.W. (1989). Radiation and light measurements. In: Pearcy, J. Ehleringer, H.A. Mooney, and P.W. Rundel (eds). *Plant Physiological Ecology: Field Methods and Instrumentation*. Chapman and Hall. New York. pp. 95-116.
- Rich, P.M. 1990. Characterizing plant canopies with hemispherical photography. In: N.S. Goel and J.M. Norman (eds). *Instrumentation for studying vegetation canopies for remote sensing in optical and thermal infrared regions*. *Remote Sensing Reviews* 5:13-29.
- UO (2007). Solar Radiation Monitoring Laboratory. Retrieved July 2017 from <http://solardat.uoregon.edu>.
- Würfel, P. (2005). *The Physics of Solar Cells*. Weinheim: Wiley-VCH. ISBN 3-527-40857-6.